Biophysical Studies on the Full-Length Human Cyclin A 2 : Protein Stability and Folding/Unfolding Thermodynamics

ARTICLE *in* THE JOURNAL OF PHYSICAL CHEMISTRY B · AUGUST 2008

Impact Factor: 3.3 · DOI: 10.1021/jp712026m · Source: PubMed

3 AUTHORS, INCLUDING:

Xiaohui Wang
Chinese Academy of Sciences
40 PUBLICATIONS **1,071** CITATIONS

SEE PROFILE

Biophysical Studies on the Full-Length Human Cyclin A_2: Protein Stability and Folding/Unfolding Thermodynamics

Xiaohui Wang, Jinsong Ren, and Xiaogang Qu*

Division of Biological Inorganic Chemistry, Key Laboratory of Rare Earth Chemistry and Physics, Changchun Institute of Applied Chemistry, Graduate School of the Chinese Academy of Sciences, Chinese Academy of Sciences, Changchun, Jilin 130022, P. R. China

Received: August 17, 2007; Revised Manuscript Received: April 19, 2008

Human cyclin A_2 participates in cell cycle regulation, DNA replication, and transcription. Its overexpression has been implicated in the development and progression of a variety of human cancers. However, cyclin A_2 or its truncated form is very unstable in the absence of binding partner, which makes it difficult to get a deep insight of structural basis of the interactions. Therefore, biophysical studies of the full-length human cyclin A_2 would provide important information regarding protein stability and folding/unfolding process. To the best of our knowledge, these have not been reported. In this report, we found that cyclin A_2 stability depended on pH, salt concentration, and denaturant concentration, and low concentration denaturant increased cyclin A_2 stability studied by UV melting, fluorescence spectroscopy, limited proteolysis, and circular dichroism. The therrmal unfolding/folding process could be described by Lumry−Eyring model: N ↔ I → D, followed by decreasing α-helix content and forming intermolecular antiparallel pleated β-sheet structures in the aggregate. Our results are of importance for studying the interactions between cyclin A_2 and therapeutic agents, such as small molecules or peptides, because cyclin A_2 is very unstable in the absence of its biological associated kinases.

Introduction

Cyclin A_2 is a hydrophobic globular protein having 432 amino-acid residues[1] and a molecular mass of 49 400. The X-ray crystallographic structure of truncated cyclin A_2 (171-432) shows strikingly high α-helix content.[2] It accumulates steadily during G2 and is abruptly destroyed just before the metaphase−anaphase transition by ubiquitin-mediated proteolysis, and it plays a critical role in cell-cycle regulation by binding and activating cyclin dependence kinase 2 (CDK2) or CDK1, thus promoting both cell-cycle G1/S and G2/M transitions.[3–7] It also participates in DNA replication and transcription.[5,8] Increased expression of cyclin A_2 has been detected in many types of cancers including breast cancer, liver cancer, lung cancer, soft tissue sarcoma, leukemia, and lymphoma.[9] Its expression level in many types of cancers appears to be of prognostic value such as prediction of aggressiveness, survival, or early relapse.[10–12]

CDK2 inhibition has the potential to be a selective cancer therapeutic strategy.[13] Small molecule CDK inhibitors such as flavopiridol and short peptides have been developed.[13,14] However, recent studies question whether selective CDK2 inhibition is a useful cancer-treatment strategy.[15,16] Additionally, Barbacid has shown no cell-cycle abnormalities either in a CDK2 null mouse or following acute ablation of CDK2 in primary cells, thereby raising the question of the real importance of CDK2 in cellular proliferation.[17] Fine has demonstrated that cyclin A_2 and/or cyclin A_2−CDK2 complex but not CDK2 is a promising anticancer target with a high therapeutic index.[18] Thus, it is of great importance for the identification of small molecules that specifically bind to cyclin A_2 and induce its conformation change so that it diminishes its affinity to bind to its associated kinases and hence inhibit their activities. However, cyclin A_2 or its truncated form (173-432) is very unstable in the absence of binding partner,[19,20] which makes it difficult to get a deep insight of the structural basis of the interactions.

To get a better understanding of cyclin A_2−ligand interaction, we characterize the biophysical and biochemical properties of cyclin A_2 in the present work. The results indicate that the chemical denaturation process can be analyzed by the two-state model, and thermal unfolding/folding can be described by Lumry−Eyring model: N ↔ I → D. To the best of our knowledge, this is the first report that systematically characterizes the biophysical properties of full-length human cyclin A_2.

Experimental Methods

Chemicals. Analytical grade 1-anilinonaphthalene-8-sulfonic acid (ANS), thioflavin-T (ThT), sodium chloride, and sodium iodine were from Sigma Chemical Co. (St. Louis, MO); ultrapure guanidine hydrochloride (GdmHCl) and urea were from USB Corporation. These reactants were used without further purification. Full-length human cyclin A_2 was prepared according to ref 21.

Electrophoresis. Sodium dodecyl sulfate polyacrylamide gel electrophoresis (SDS-PAGE) was carried out as described by Laemmli by using a 12% gel.[22] All gels were stained by Coomassie Brilliant Blue G-250 staining solution (0.1% Coomassie Brilliant Blue G-250, 4% H_3PO_4, 10% $(NH_4)_2SO_4$, 20% ethanol).

Fluorescence Measurements. Measurements of fluorescence were taken in a Jasco FP6500 spectrofluorometer by using a 1 cm path length quartz cuvette. The slits were set at 5 and 10 nm for excitation and emission, respectively. For intrinsic tryptophan fluorescence measurements, the excitation wavelength of 290 nm was used to avoid excitation of tyrosine, whereas for the extrinsic ANS and ThT fluorescence measurements, the excitation wavelengths were 380 and 440nm, respectively. Appropriate blank spectra were recorded on the

* Corresponding author. E-mail: xqu@ciac.jl.cn.

10.1021/jp712026m CCC: $40.75
Published on Web 06/24/2008

buffer components and subtracted from spectra obtained on the samples. Fluorescence was also corrected by the relation, $F_{corr} = F_{obs}$ antilog $(OD_{ex} + OD_{em}/2)$ for the inner filter effect when necessary, where OD_{ex} and OD_{em} are the optical densities at excitation and emission wavelengths, respectively.[23]

For energy-transfer experiments, the efficiency of energy transfer (EET) from tryptophan to ANS was calculated from the formula, $EET = 1 - (F_t/F_0)$, where F_t and F_0 are the relative fluorescence intensities of energy donor (tryptophan) in the presence and the absence of energy acceptor (ANS), respectively. According to the Forester theory,[24] a critical distance R_0, at which the energy-transfer efficiency is 0.5, can be found for any given donor−acceptor couple from the following formula

$$R_0^6 = \frac{9000(\ln 10)k^2 Q_D}{128\pi^5 N n^4}\int_0^\infty F_D(\lambda)\epsilon_A(\lambda)\lambda^4\,d\lambda$$

where Q_D is the quantum yield of the donor in the absence of acceptor, N is the Avogadro number, n is the refractive index of the medium, $F_D(\lambda)$ is the normalized fluorescence intensity of the donor, $\varepsilon_A(\lambda)$ is the extinction coefficient wavelength function of the acceptor, and k^2 is a factor describing the relative spatial orientation of the transition dipoles of the donor and the acceptor, usually assumed to be 2/3, corresponding to freely rotating dipoles. When EET and R_0 have been estimated, an average donor−acceptor distance R can be derived according to the following relationship:

$$R = R_0\left(\frac{1}{EET} - 1\right)^{1/6}$$

The quenching of tryptophan fluorescence upon the addition of ANS was analyzed according to the equation

$$\log\left(\frac{F_0}{F} - 1\right) = -\log K_d + n\log[\mathrm{ANS}]$$

where F_0 and F denote the observed fluorescence in the absence and presence of the ANS, respectively, and n is the number of binding sites per protein molecule.[25] The data of titration of cyclin A_2 with ANS were fit to a hyperbolic function, with the measured fluorescence intensity = ([ANS] × fluorescence maximum)/([ANS] + K_d). Scatchard-like plots were prepared by assuming that nearly all of the ANS was in an unbound form and that all bound ANS molecules had the same fluorescence. Hence, bound/free was represented as fluorescence intensity divided by total ANS concentration.

Unfolding by Urea and Guanidine Hydrochloride. Samples for spectroscopic measurements were diluted into buffer A containing indicated concentration of GdmHCl or urea. All spectral measurements were taken at 25 °C. Sample solutions were prepared 12−16 h prior to taking measurements. Preliminary experiments revealed a time-dependent change in fluorescence intensity after preparation of the sample. Most of the fluorescence changes occurred in the first hour and occurred more rapidly in samples containing urea or GdmHCl; there was no detectable change in measurements taken after 12 h.

By using a nonlinear least-squares method, the entire data ($Y_{[d]}$, $[d]$) of each denaturant-induced transition curve were analyzed by the linear extrapolation method (LEM) for $\Delta G^o_D(H_2O)$ and m_d by using the relation

$$Y(\mathrm{D}) = \frac{Y_N(\mathrm{d}) + Y_D(d)\exp[-(\Delta G^o_D(H_2O) + m_d[d])/RT]}{1 + \exp[-(\Delta G^o_D(H_2O) + m_d[d])/RT]}$$

where $Y(d)$ is the observed optical property intensity at $[d]$, the molar concentration of GdmHCl or urea, $Y_N(d)$ and $Y_D(d)$ are the observed optical property intensity of the native and denatured protein molecules under the same experimental conditions in which $Y(d)$ was measured, respectively, $\Delta G^o_D(H_2O)$ is the value of the Gibbs energy change in the absence of the denaturant, m_d is the slope $(\partial\Delta G_D/\partial[d])$, R is the universal gas constant, and T is the temperature in Kelvin.[26] It should, however, be noted that the analysis of denaturant-induced transition curves was done by assuming that unfolding is a reversible two-state process, and $[d]$-dependencies of $Y_N(d)$ and $Y_D(d)$ are linear (i.e., $Y_N(d) = a_N + b_N[d]$ and $Y_D(d) = a_D + b_D[d]$, where a and b are $[d]$-independent parameters, and subscripts N and D represent these parameters for the native and denatured protein molecules, respectively).

The change in solvent-accessible surface area upon unfolding (ΔASA, Å^2) is determined by the equations[27] m_{urea}(cal mol^{-1} M^{-1}) = 368 + 0.11(ΔASA) or m_{GdmHCl}(cal mol^{-1} M^{-1}) = 953 + 0.23(ΔASA). Data were also analyzed with the denaturant binding model (DBM) by using the relation

$$\Delta G^o_D = \Delta G^o_D(H_2O) - \Delta nRT\ln(1 - ka)$$

where Δn is the difference in the number of denaturant binding sites for denatured and native conformations, k is the equilibrium constant for each site, and a is the activity of the denaturant.[28] Activities of urea and GdmHC1 are obtained from the equations $a_{urea} = 0.9815[d] - 0.02978[d]^2 + 0.00308[d]^3$ and $a_{GdmHCl} = 0.6761[d] - 0.1468[d]^2 + 0.02475[d]^3 - 0.00132[d]^4$, respectively.[28,29]

Fluorescence Quenching Experiments. Quenching of intrinsic tryptophan fluorescence by iodide or acrylamide was examined in buffer A with indicated concentrations of urea or GdmHCl. A small amount of $Na_2S_2O_3$ was added to the iodide solutions to prevent I^{3-} formation. Estimates of the dynamic and static quenching constants for acrylamide were obtained by fitting the hyperbolic form of the Stern−Volmer equation to the data, which includes an exponential term to account for static quenching

$$\frac{F_0}{F}e^{-\nu[X]} = 1 + K_{sv}[\mathrm{X}]$$

where K_{sv}, the Stern−Volmer constant for collisional quenching, gives the approximate degree of exposure of tryptophan residues to the solvent, and ν, the static quenching constant, is related to the probability of finding the quencher molecule close enough to the excited chromophore to quench it with 100% efficiency.[30] Data are presented by using the inverse form of the Stern−Volmer equation as F_0/F versus [quencher]. Because iodide quenching did not have a significant static component, the exponential term was not included in fits of the equation to these data.

Thermal Denaturation. Cyclin A_2 solution in quartz cuvette was placed in a thermostatic cell holder in JASO FP-6500 spectrofluorimeter.[31,32] The cell holder was maintained at constant temperature by circulating water from a constant temperature water bath. The tubings connecting the water bath to the cell holder were insulated to minimize heat loss. After a set temperature was reached, the sample was equilibrated for 10 min to attain the temperature before an emission spectrum was collected. Both intrinsic tryptophan and extrinsic ANS and ThT fluorescence spectra were collected for each temperature.

Thermal denaturation was also monitored by absorbance at 280 nm (mainly reflecting turbidity at high temperature due to aggregation) on a JASCO V-550 spectrophotometer equipped with a peltier temperature controller.[32,33] Apparent temperature transition values (T_{trs}, app) were determined[32,33] by differentiation of melting profiles by using the Origin7.5 software (OriginLab Corporation, Northampton, MA).

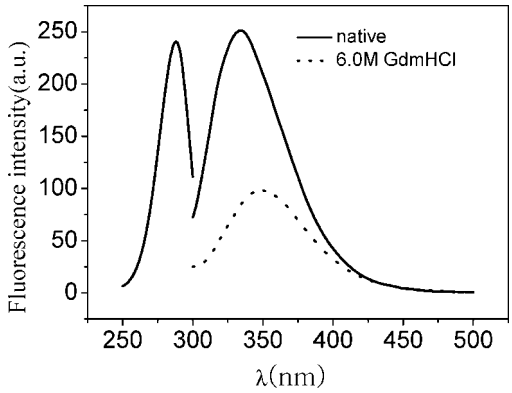

Figure 1. Fluorescence spectra of cyclin A_2.The excitation (250−300 nm) and emission (300−500 nm) spectra of cyclin A_2 were recorded by using $\lambda_{em} = 333$ nm and $\lambda_{exc} = 290$ nm, respectively. Protein concentration was 1.0 μM in buffer A without or with 6 M GdmHCl.

We also employ circular dichroism (CD) in the analysis of the unfolding of cyclin A_2 as a spectroscopic probe which is sensitive to protein secondary structure.[34] CD spectra[31,32] and CD melting[33,34] experiments were measured on a JASCO J-810 spectropolarimeter equipped with a temperature-controlled water bath. CD melting was monitored by ellipticity at 222 nm.[33,34] The optical chamber of CD spectrometer was deoxygenated with dry purified nitrogen (99.99%) for 45 min before use and kept under nitrogen atmosphere during experiments. Four scans were accumulated and automatically averaged. Scan speed was set to 10 nm/min with 4 s response time, 0.1 nm data pitch, and 1 nm bandwidth.

Fourier-Transformed Infrared Spectroscopy (FTIR). All the spectra were recorded on a Bruker Vertex 70 FT-IR Spectrometer[21] with OPUS Vertex 70 software 5.0 (Bruker Optics Inc.). Protein solution and thermal aggregate were analyzed by a Pike Technologies ZnSe horizontal attenuated total reflection unit. Each spectrum comprised 1024 scans measured at a spectral resolution of 2 cm^{-1} in the 4000−600 cm^{-1} range. When necessary, the spectra were corrected for water vapor and H_2O contribution to obtain a flat baseline between 2300 and 1850 cm^{-1}. All the absorbance spectra were normalized to correct for concentration-dependent effects, and the second derivative of amide band I spectra was used to determine the frequencies at which the different spectral components were located.

Limit Trypsin Digestion. The enhanced stability effect of low concentration denaturant on human cyclin A_2 was also evaluated by limit trypsin proteolysis.[34] Briefly, 10 μg aliquots of the human cyclin A_2 were equilibrated at 25 °C in the presence of 0.6 M urea under test. Then, 20 ng trypsin was added, and digestion was allowed to proceed at 25 °C for different times. At the end of trypsin digestion, samples were added with an equal volume of SDS-PAGE reducing sample buffer, heated at 95 °C for 3 min and subjected to 12% SDS-PAGE.

Results and Discussion

Examination of Protein Unfolding by Intrinsic Tryptophan Fluorescence. Cyclin A_2 has 17 tyrosines and three tryptophans. After excitation at 260 nm, where tyrosyl side chains are selectively excited, or at 290 nm, where the tryptophyl side chains are selectively excited, the fluorescence spectra have maxima at 333 ± 1 nm (Figure 1), which is typical for buried tryptophyl side chains in nonpolar environment. The absence of tyrosyl emission in the fluorescence spectra of the cyclin A_2 after excitation at 260 and 290 nm can be explained by a singlet−singlet radiation-less energy transfer from phenol groups (donors) to indole rings (acceptors).[24] The X-ray model of cyclin A_3 demonstrates many possibilities for an efficient Tyr to Trp energy transfer.[2]

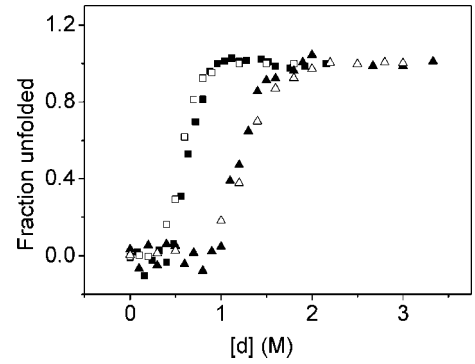

Figure 2. Unfolding equilibrium curves of cyclin A_2 as a function of GdmHCl (square) or urea (triangle) measured by intrinsic tryptophan fluorescence at 333 nm (open) or CD ellipticity at 222 nm (filled).

TABLE 1: Thermodynamic and Conformational Parameters Associated with Urea and GdmHCl Induced Denaturation of Cyclin A_2 in Buffer A at 25 °C Monitored by Fluorescence

denaturant	$\Delta G^o_D(H_2O)$ (kJ mol^{-1}) DBM	$\Delta G^o_D(H_2O)$ (kJ mol^{-1}) LEM	m_d (kJ mol^{-1} M^{-1})	C_m (M)	ΔASA[a] (Å^2)
Urea	16.06 ± 1.40	16.38 ± 2.82	−13.00 ± 1.98	1.28	24881
GdmHCl	16.25 ± 1.57	16.81 ± 3.04	−31.15 ± 4.23	0.54	28204

[a] ΔASA values were calculated according to ref 27.

Unfolded states of protein play an important role in protein folding, transport across membranes, and proteolysis, which is the reason for the increasing interest in these states during the past years.[35] Cyclin A_2 can shuttle between the nucleus and the cytoplasm.[36] The unfolding reaction in the presence of GdmHCl or urea was followed by fluorescence and CD measurements.

Reversibility of isothermal unfolding/folding was confirmed by matching the optical property before denaturation by GdmHCl or urea and after renaturation (Figure S1 in Supporting Information). With both chaotropic agents, there were no apparent changes in fluorescence intensity at relative low concentrations of denaturant followed by a slightly red shift in the emission wavelength and a reduction in fluorescence intensity at higher concentrations. The addition of NaCl to 0.5 M in the absence of GdmHCl did not induce a decrease in fluorescence intensity as was observed at 0.5 M GdmHCl, indicating that the effect at this concentration of GdmHCl is not related to ionic strength or to the presence of chloride ions. As shown in Figure 2, unfolding equilibrium curves of cyclin A_2 as a function of GdmHCl or urea monitored by intrinsic tryptophan fluorescence at 333 nm and CD ellipticity at 222 nm are superimposed within experimental error. The unfolding free energy changes of two denaturants, whether determined by LEM or DBM, were identical within error, suggesting that the free energy change is a property of the protein system and independent of the denaturant (Table 1). This appears to be consistent with the two-state hypothesis in which $\Delta G^o_D(H_2O)$ is a thermodynamic function of state.[37,38] Large positive values of ΔASA for the process indicate the importance of exposure of hydrophobic residues due to protein unfolding.

ANS Binding. ANS, a kind of naphthalene-based probes, is often used as a probe of the extent of exposure of hydrophobic

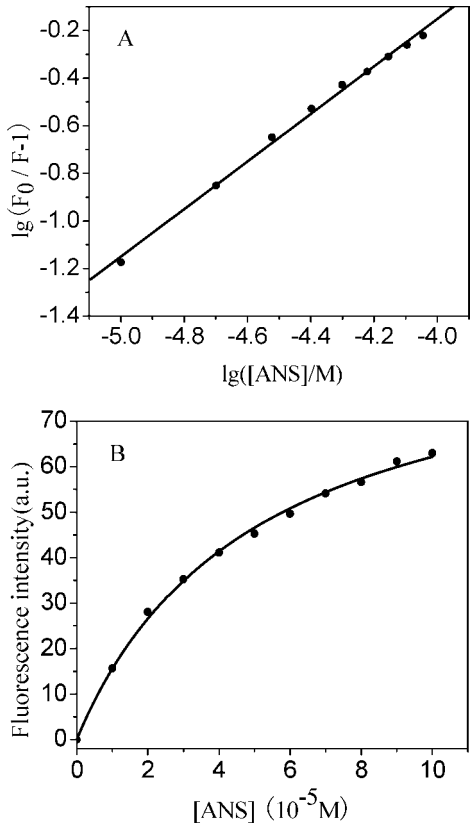

Figure 3. Concentration dependence of energy transfer between tryptophan and ANS. Protein concentration was 1.0 μM in buffer A. The excitation wavelength was 290 nm. (A) Effect of increasing ANS concentration on tryptophanyl emission intensity. The fluorescence intensity was monitored at 333 nm and is expressed as $\log(F_0/F - 1)$. (B) ANS concentration dependence of energy transfer between tryptophan and bound ANS. The emission was measured at 475nm.

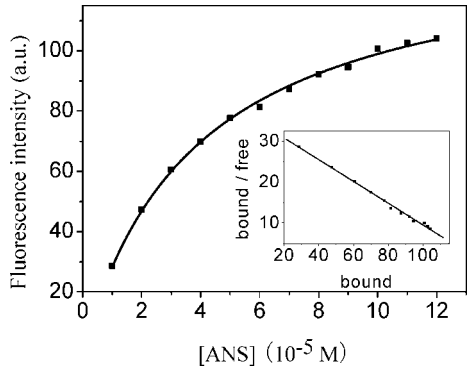

Figure 4. Binding of cyclin A_2 at different concentrations of ANS. Cyclin A_2 was at 1.0 μM in buffer A. The excitation wavelength was 380 nm, and the increase in ANS fluorescence was monitored at a fixed wavelength of 475nm. All measurements were taken at room temperature. The solid line represents the hyperbolic fit to the data (open circles). Inset is Scatchard-like transformation of the data (filled circle).

regions of the protein.[39] When ANS bound to native cyclin A_2, its fluorescence maximum was considerably blue-shifted, that is, from 515 nm in water to 475 nm. At the same time, the intrinsic protein emission was strongly quenched by resonance energy transfer from tryptophanyl residues to ANS (Figure 3). Titration of cyclin A_2 with ANS gave a hyperbolic plot as shown in Figure 4. The titration data transformed as Scatchard plot is linear, consistent with a single type of binding site hypothesis. A n value of 1.00 was obtained by the analysis of tryptophan quenching data, suggesting there is only one ANS binding site per protein molecule. The average tryptophan−ANS distance $R = 2.52$ nm was derived from Forester resonance energy transfer theory.

For cyclin A_2, there are three tryptophans: W90, W217, and W372. W90 is located at the cyclin A_2 N-terminal responsible for ubiquitin-dependence of proteolysis; W372 is located at the hinge region of the second cyclin box not responsible for CDK binding; and W217 is in the cyclin-binding groove which is formed by a shallow hydrophobic surface cleft and involves initial recognition of the substrates and inhibitors of the competent CDK2-cyclin A_2 complex, such as pRb, E2F-1, $p21^{WAF1}$ and $p27^{KIP1}$. X-ray data also show that W217 makes hydrophobic interaction with ZRXL cyclin binding motif.[40] One requirement for the resonance interaction to produce energy transfer is that the two fluorophores, that is, the donor (tryptophan) and the acceptor (ANS), be within a certain distance.[20] Therefore, it is most likely that the only ANS binding site of human cyclin A_2 is located at the cyclin binding groove.

Thermal Denaturation. The absorption spectrum of cyclin A_2 shows a band with maximum at 278 nm, typical for proteins containing aromatic amino acids. Thermal induced denaturation of cyclin A_2 was irreversible. This is evident from the rescan of the thermally denatured protein after cooling down that is void of the sigmoidal transition.

As shown in Figure 5A, thermal transition of cyclin A_2 was concentration dependent. When cyclin A_2 concentration was 0.12 μM, there was no apparent fluorescence change during thermal denaturation.

The decrease in tryptophan fluorescence intensity with increasing temperature was shown in Figure 5B, which showed a transition at about 45 °C. It is interesting to note here that the polarity of the environment of tryptophan as reflected in the fluorescence emission maximum (λ_{max}) did not change with the temperature of human cyclin A_2 solution. This observation indicates that cyclin A_2 is not fully unfolded at the end of heat denaturation. It is most likely that the high temperature perturbs cyclin A_2 native conformation to a certain degree to promote aggregation so that it prevents cyclin A_2 from completely unfolding. Hence, the mechanism of cyclin A_2 heat denaturation may be described by Lumry−Eyring model: N ↔ I → D,[41,42] where N is the native conformation, I is intermediate state that is partially unfolded and much more prone to aggregation than both native and completely unfolded conformations, and D is the denatured state (oligomer or aggregate).

ThT is a benzothiazole dye that specifically interacts with β-pleated sheet of amyloid fibrils. When this dye binds to amyloid fibrils, there is a large enhancement in the fluorescence intensity of ThT relative to free dye.[43,44] ANS is a hydrophobic fluorescence probe that has been immensely useful in identification of partially folded intermediates in the denaturation/refolding pathways of the proteins.[45] To further characterize the process of heat denaturation, we employed ANS and ThT fluorescence to monitor the exposure of hydrophobic patches of partially folded intermediates and to identify aggregate formation, respectively. Both ANS and ThT fluorescence intensities show little variation with temperature below 35 °C (Figure 5C). Above this temperature, the fluorescence intensities increase, reaching a maximum around 45 °C, which is coincident with the transition point of tryptophan fluorescence. At higher temperatures, the intensities fall down. These results confirm the proposed mechanism of cyclin A_2 heat denaturation and indicate that amyloid-like aggregate forms during thermal denaturation.

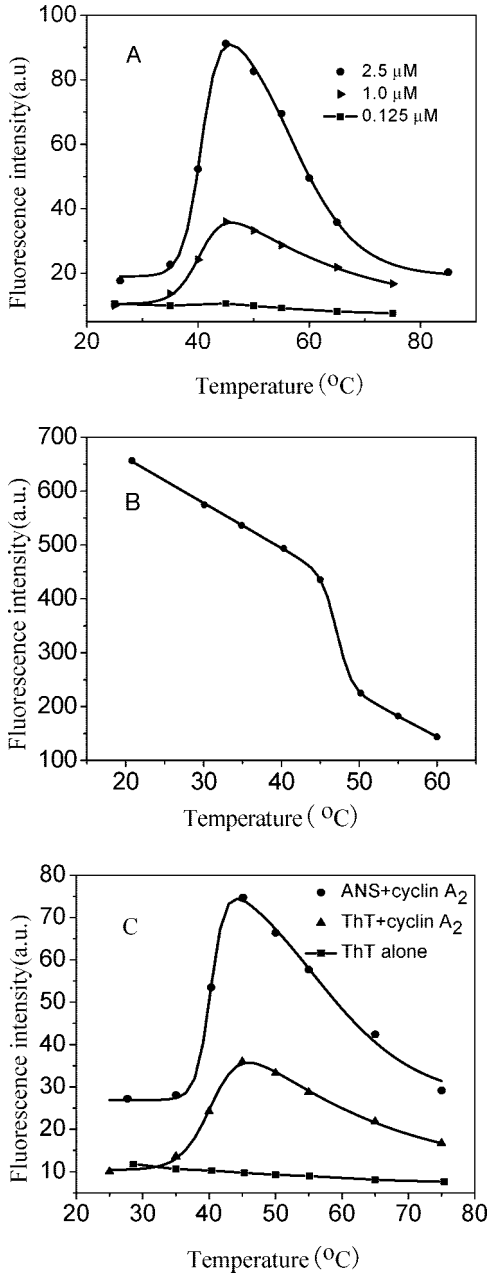

Figure 5. Fluorescence intensity as a function of temperature. (A) protein-concentration dependence of ThT fluorescence enhancement. ThT concentration is 10 μM. The fluorescence intensity was monitored at 482 nm. (B) Intrinsic tryptophan fluorescence intensity as a function of temperature. Cyclin A_2 is 1.0 μM in buffer A. The fluorescence intensity was monitored at 333 nm. (C) Extrinsic ANS and ThT fluorescence intensity as a function of temperature in 1.0 μM cyclin A_2 solution. ThT or ANS is 10 μM.

FTIR spectroscopy of thermal aggregate of cyclin A_2. FTIR spectroscopy has proved to be a powerful tool to investigate structural information of protein aggregate.[21,46,47] To further determine whether thermal aggregate of cyclin A_2 has amyloid-like intermolecular pleated β-sheet structures, we employed FTIR to study the secondary structure. As shown in Figure 6, the FTIR spectrum of native cyclin A_2 in the amide region I was dominated by a peak at 1655 cm^{-1} that arises from C═O vibrations in α helices. Minor peaks were distinguished at 1630, 1642, and 1660 cm^{-1}, usually assigned to parallel β sheet, random, and turn conformations, respectively. The FTIR of cyclin A_2 thermal aggregate was completely different. The peak corresponding to α helices decreased significantly, and a

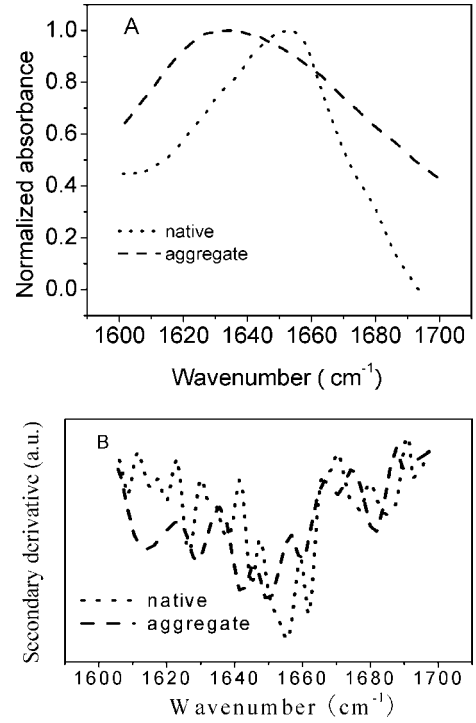

Figure 6. Unresolved (A) and second derivative (B) FTIR spectra of native form and thermal aggregate of cyclin A_2.

strong peak was detected at 1626 cm^{-1}. This band, together with the presence of a band at 1682 cm^{-1}, is indicative of newly formed, extended intermolecular antiparallel pleated β-sheet structures in the aggregate.[46] Interestingly, decrease in α-helix content and increase in β-sheet content were detected in thermal aggregate in comparison to its native protein. These results confirm that cyclin A_2 thermal aggregate has an amyloid fibril-like structure.

Effect of Salt Concentration, pH, and Low-Concentration Denaturant on the Stability of Cyclin A_2. Cyclin A_2 is a hydrophobic protein that tends to aggregate over time in the absence of its binding partners.[19,20] According to Bowman, truncated cyclin A_2 (173-432) is both unfolding and aggregating[19] at temperatures above 25 °C. In our cyclin A_2 preparation process, we found that purified full-length cyclin A_2 was prone to aggregate when stored in 20 mM Tris, 0.1 M NaCl (pH 8.0) or PBS buffer at 4 °C. To formulate appropriate buffer for cyclin A_2, we evaluated salt concentration, pH, and low-concentration denaturant on the stability of cyclin A_2.

As shown in Figure 7A, stability is affected by changes in the NaCl concentration. At concentrations of 0.05−0.7 M NaCl, the temperature of transition steeply increased from 43 to 62 °C. This temperature decreased at concentrations > 0.7 M NaCl, and at 1.5 M NaCl, the temperature of transition was 50 °C. Compared to the effect of salt concentration, pH has little effect on the stability of cyclin A_2 (Figure 7B). Hence, buffer A (20 mM Tris, 0.5 M NaCl, pH 8.0) is chosen as working solution to prevent aggregation. Cyclin A_2 appears to be stable when stored under these conditions at 4 °C for at least a month.

At low concentration of denaturant in our experimental conditions, there are no apparent changes in intrinsic tryptophan fluorescence intensity or CD ellipticity (Figure S2 in Supporting Information). For GdmHCl, an increase in the temperature of transition from 59 to 76 °C in the concentration range 0−0.2 M was observed (Figure 8A); for urea, an increase in the temperature of transition from 59 to 80 °C in the concentration range 0−0.6 M was observed (Figure 8B). It seems that low-

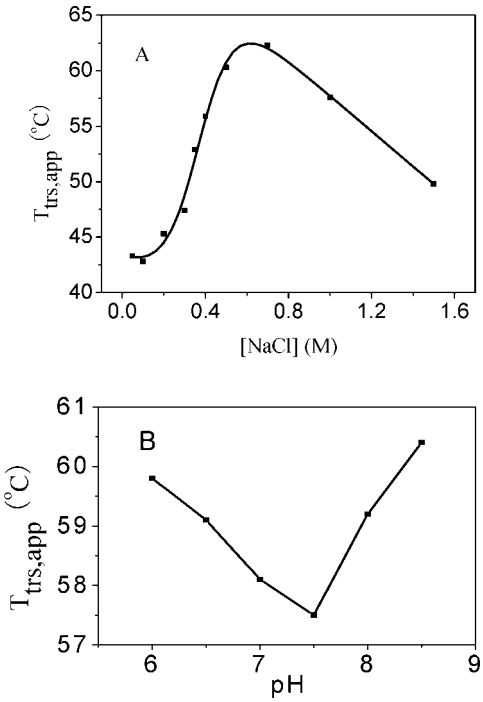

Figure 7. Effects of salt concentration (A) and pH (B) on the thermal stability of cyclin A_2.

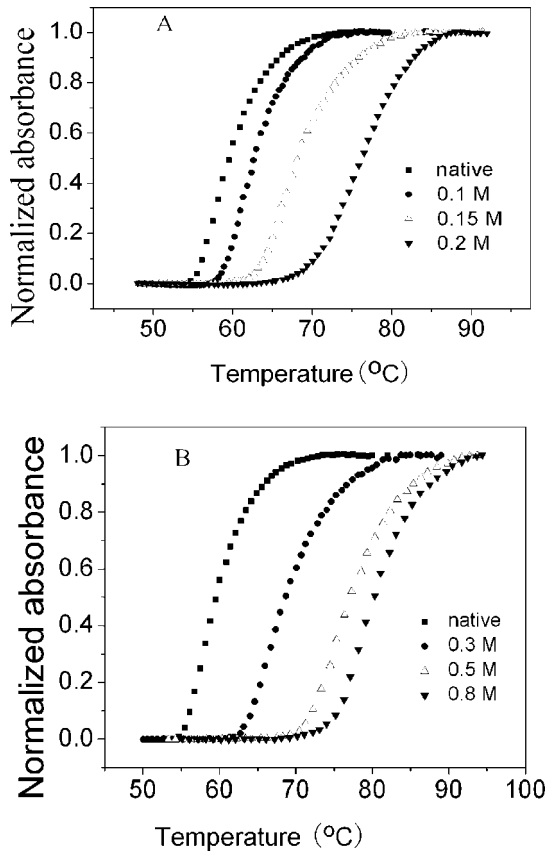

Figure 8. Effect of low-concentration GdmHCl (A) and urea (B) on thermal stability of cyclin A_2. Protein concentration was 1.0 μM in buffer A with indicated concentration of denaturant.

concentration denaturant enhances cyclin A_2 stability. These observations contradict the general notion that denaturant decreases protein stability as a result of the chaotropic effect. To further investigate this effect, fluorescence quenching, limited proteolysis, and CD melting experiments have been carried out.

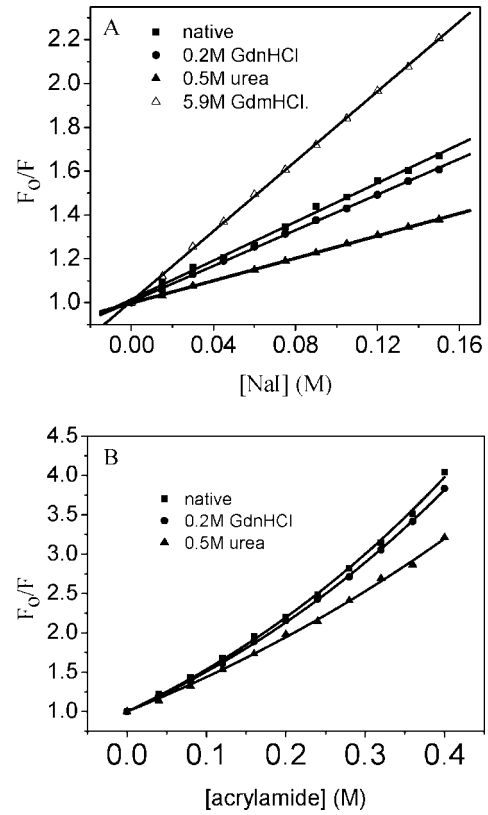

Figure 9. Stern−Volmer plots for fluorescence quenching with (A) NaI and (B) acrylamide performed at room temperature after excitation of the samples at 290nm. Plot for quenching at 5.9 M GdmHCl with acrylamide is not shown in the figure to clarify the total profile.

TABLE 2: Quenching Constants for Cyclin A_2 under Different Conditions

	acrylamide		NaI
condition	K_{sv} (M^{-1})	ν (M^{-1})	K_{sv} (M^{-1})
native	3.60 ± 0.25	1.22 ± 0.11	4.43 ± 0.09
0.2 M GdmHCl	3.34 ± 0.13	1.23 ± 0.06	4.07 ± 0.04
0.5 M Urea	3.26 ± 0.23	0.82 ± 0.11	2.56 ± 0.02
5.9 M GdmHCl	4.03 ± 0.65	4.65 ± 0.27	8.0 ± 0.04

Examination of Tryptophan Exposure by Fluorescence Quenching. Fluorescent quenching has been widely used for studying the degree of exposure and environment of aromatic amino acid residues.[48] Acrylamide is an efficient neutral quencher of tryptophyl fluorescence and can penetrate the protein matrix. In contrast, the ionic quenchers are hydrated and cannot diffuse into the protein molecule. To probe the modification of tryptophan micro-environment of cyclin A_2 at low-concentration denaturant, we examined iodide and acrylamide quenching of tryptophan fluorescence.

Cyclin A_2 gave linear Stern−Volmer plots with iodide, the slopes of which decreased at low concentration of GdmHCl (0.2 M) or urea (0.5 M), shown in Figure 9A. Quenching by acrylamide gave a similar pattern of decreased quenching upon addition of low concentration of GdmHCl or urea (see Figure 9B) but exhibited both static and dynamic components as indicated by the upward curvature in the Stern−Volmer plots. The quenching studies, summarized in Table 2, indicate that cyclin A_2 at low-concentration denaturant adopts a more compact conformation that decreases the solvent accessibility of aromatic amino acids, although there are no apparent changes of tryptophan fluorescence at 0.2 M GdmHCl or 0.5 M urea.

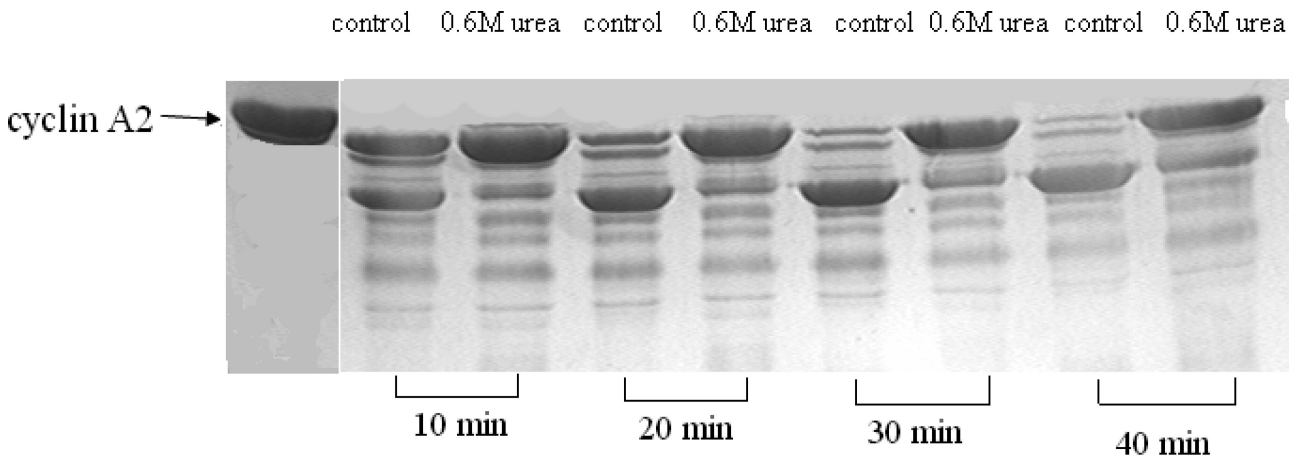

Figure 10. Low-concentration denaturant enhances the stability of cyclin A_2 against trypsin proteolysis. Aliquots (10 μg) of the cyclin A_2 were incubated at 25 °C with trypsin in the absence or in the presence of 0.6 M urea for varying times.

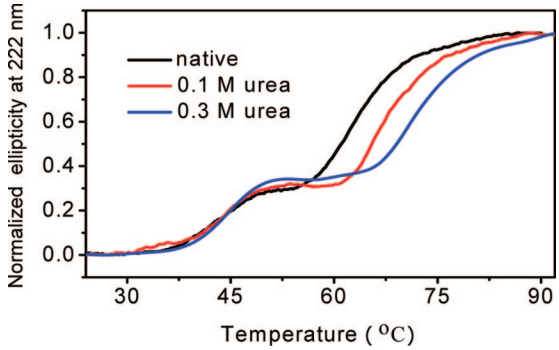

Figure 11. CD melting profiles of cyclin A_2 at low-concentration denaturant. Protein concentration was 1.0 μM in buffer A with indicated concentration of denaturant. Ellipticity of cyclin A_2 at 222 nm was monitored on a Jasco J-810 spectropolarimeter with increasing temperature.

Probing the Conformational Flexibility of Human Cyclin A_2 at Low-Concentration Denaturant by Limited Proteolysis. To corroborate the results of the heat denaturation and fluorescence quenching studies indicating that the low-concentration denaturant enhances cyclin A_2 stability, we examined limited trypsin proteolysis,[34] which is a very sensitive probe of protein structure and chain flexibility.

As shown in Figure 10, cyclin A_2 at low-concentration urea is less susceptible to trypsin digestion, which is suggestive of the more rigid and compact conformation that it assumes at 0.6 M urea. This is consistent with the results of fluorescence quenching experiment. Trypsin retains 100% enzyme activity at 0.6 M urea; therefore, we can eliminate the possibility that the higher resistance to limited proteolysis is due to the inhibition of trypsin activity.

CD Melting and Protein Unfolding. Fluorescence quenching and limited proteolysis results indicate that cyclin A_2 at low-concentration denaturant adopts a more compact and rigid conformation and may form partially unfolding immediate, which can be stabilized by the denaturants and prevents aggregation during thermal denaturation process. This was further studied by CD meltings (Figure 11). There are two transitions observed in CD melting profiles of cyclin A_2 by monitoring protein-backbone CD change through ellipticity at 222 nm, which is more sensitive than monitoring chromophore-absorbance change at 280 nm in UV melting. The first transition may correspond to N ↔ I transition because the transition temperature is at 44 °C, consistent with the transition temperature observed in fluorescence measurements during thermal denaturation (Figure 5). This was not observed in UV melting by monitoring chromophore-absorbance change at 280 nm and indicates that chromophore-absorbance change at 280 nm is not sensitive to the partial unfolding from N ↔ I transition. The second transition corresponds to I → D transition, which was also observed in UV melting. Low concentration of denaturant hardly changes the first transition temperature (T_{trs1} = 44 °C), however, significantly increases the second transition temperature (T_{trs2} from 62 to 78 °C). This demonstrates that low-concentration denaturant can stabilize the partially unfolding immediate and prevent aggregation.

In summary, protein stability and folding/unfolding thermodynamics of the full-length human cyclin A_2 have been studied. Our results show that cyclin A_2 stability depends on pH, salt concentration, and denaturant concentration. Low-concentration denaturant can increase cyclin A_2 stability. Chemical denaturant-induced unfolding/folding can be analyzed by the two-state model. The thermal folding/unfolding process can be described by Lumry−Eyring model, N ↔ I → D, and followed by decreasing α-helix content and forming intermolecular antiparallel pleated β-sheet structures in the aggregate. All these results would be of importance for studying cyclin A_2 binding to therapeutic agents, such as small molecules or peptides, because cyclin A_2 is very unstable in the absence of its biological associated kinases.

Acknowledgment. The authors thank the referees' helpful comments. This project was supported by NSFC, Funds from the Chinese Academy of Sciences and Jilin Province.

Supporting Information Available: Supporting figures. This information is available free of charge via the Internet at http://pubs.acs.org.

References and Notes

(1) Pines, J.; Hunter, T. *Nature* **1990**, *346*, 760–763.
(2) Brown, N. R.; Noble, M. E. *Structure* **1995**, *15*, 1235–1247.
(3) Swenson, K. I.; Farrell, K. M.; Rudweman, J. V. *Cell* **1986**, *47*, 861–870.
(4) Lehner, C. F.; P. H. O'Farrell, P. H. *Cell* **1989**, *56*, 957–968.
(5) Pagano, M.; Pepperkok, R.; Verde, F.; Ansorge, W.; Draetta, G. *EMBO J.* **1992**, *11*, 961–971.
(6) Murray, A. *Cell* **1995**, *81*, 149–152.
(7) Glotzer, M.; Murray, A. W.; Kirschner, M. W. *Nature* **1991**, *349*, 132–138.
(8) Kim, T. Y.; Kaelin, W. G., Jr *Mol. Biol. Cell* **2001**, *12*, 2207–2217.

(9) Yam, C. H.; Fung, T. K.; Poon, R. Y. *Cell. Mol. Life Sci.* **2002**, *59*, 1317–1326.
(10) Mrena, J.; Wiksten, J. P.; Kokkola, A.; Nordling, S.; Haglund, C.; Ristimaki, A. *Int. J. Cancer* **2006**, *119*, 1897–1901.
(11) Husdal, A.; Bukholm, G.; Bukholm, I. R. *Cell. Oncol.* **2006**, *28*, 107–116.
(12) Aaltonen, K.; Ahlin, C.; Amini, R. M.; Salonen, L.; Fjallskog, M. L.; Heikkila, P.; Nevanlinna, H.; Blomqvist, C. *Br. J. Cancer* **2006**, *94*, 1697–1702.
(13) De Azevedo, W. F., Jr.; Mueller-Dieckmann, H. J.; Schulze-Gahmen, U.; Worland, P. J.; Sausville, E.; Kim, S. H. *Proc. Natl. Acad. Sci. U.S.A.* **1996**, *93*, 2735–2740.
(14) Condeau, C.; Gerbal-Chaloin, S.; Bello, P.; Aldrian-Herrada, G.; Morris, M. C.; Divita, G. *J. Bio. Chem.* **2005**, *280*, 13793–13800.
(15) Tetsu, O.; McCormick, F. *Cancer Cell* **2003**, *3*, 233–245.
(16) Berthet, C.; Aleem, E.; Coppola, V.; Tessarollo, L.; Kaldis, P. *Curr. Biol.* **2003**, *13*, 1775–1785.
(17) Ortega, S.; Prieto, I.; Odajima, J.; Martin, A.; Dubus, P.; Sotillo, R.; Barbero, J. L.; Malumbres, M.; Barbacid, M. *Nat. Genet.* **2003**, *35*, 25–31.
(18) Chen, W.; Lee, J.; Cho, S. Y.; Fine, H.A. *Cancer Res.* **2004**, *64*, 3949–3957.
(19) Bowman, P.; Galea, C. A.; Lacy, E.; Kriwacki, R. W. *Biochim. Biophys. Acta* **2006**, *1764*, 182–189.
(20) Canela, N.; Orzáez, M.; Fucho, R.; Mateo, F.; Gutierrez, R.; Pineda-Lucena, A.; Bachs, O.; Pérez-Payá, E. *J. Biol. Chem.* **2006**, *281*, 35942–35953.
(21) Wang, X.; Fu, M.; Ren, J.; Qu, X. *Protein Expr. Purif.* **2007**, *5*−*6*, 27–34.
(22) Laemmli, U. K. *Nature* **1970**, *227*, 680–685.
(23) Borissevitch, I. E. *J. Lumin.* **1999**, *81*, 219–224.
(24) Stryer, L. *Annu. Rev. Biochem.* **1978**, *47*, 819–846.
(25) Alain, M.; Michel, B.; Michel, A. *J. Chem. Educ.* **1986**, *63*, 365–366.
(26) Moza, B.; Qureshi, S. H.; Ahmad, F. *Biochim. Biophys. Acta* **2003**, *1646*, 49–56.
(27) Myers, J. K.; Pace, C. N.; Scholtz, J. M. *Protein Sci.* **1995**, *4*, 2138–2148.
(28) Moosavi-Movahedi, A. A.; Nazari, K. *Int. J. Biol. Macromol.* **1995**, *17*, 43–47.
(29) George, P. *J. Biol. Chem.* **1953**, *201*, 413–426.
(30) Eftink, M. R.; Ghiron, R. A. *Anal. Biochem.* **1981**, *114*, 199–227.
(31) Li, X.; Peng, Y.; Qu, X. *Nucleic Acids Res.* **2006**, *34*, 3670–3676.
(32) Zhang, H.; Yu, H.; Ren, J.; Qu, X. *Biophys. J.* **2006**, *90*, 3203–3207.
(33) Li, X.; Peng, Y.; Ren, J.; Qu, X. *Proc. Natl. Acad. Sci. U.S.A.* **2006**, *103*, 19658–19663.
(34) Wu, Q.; Wang, J.; Zhang, L.; Hong, A.; Ren, J. *Angew. Chem., Int. Ed.* **2005**, *44*, 4048–4052.
(35) Dill, K. A.; Shortle, D. *Annu. Rev. Biochem.* **1991**, *60*, 795–825.
(36) Jackman, M.; Kubota, Y.; den Elzen, N.; Hagting, A.; Pines, J. *Mol. Biol. Cell* **2002**, *13*, 1030–1045.
(37) Santoro, M. M.; Bolen, D. W. *Biochemistry* **1988**, *27*, 8063–8068.
(38) Santoro, M. M.; Bolen, D. W. *Biochemistry* **1992**, *31*, 4901–4907.
(39) Sirangelo, I.; Malmo, C.; Casillo, M.; Irace, G. *Photochem. Photobiol.* **2002**, *76*, 381–384.
(40) George, K.; Andrews, M. J.; McInnes, C.; Cowan, A.; Powers, H.; Innes, L.; Plater, A.; Griffiths, G.; Paterson, D.; Zheleva, D. I.; Lane, D. P.; Green, S.; Walkinshaw, M. D.; Fischer, P. M. *Structure* **2003**, *11*, 1537–1546.
(41) Sanchez-Ruiz, J. M. *Biophys. J.* **1992**, *61*, 921–935.
(42) Roberts, C. J. *J. Phys. Chem. B* **2003**, *107*, 1194–1207.
(43) Yu, H.; Ren, J.; Qu, X. *Biophys. J.* **2007**, *92*, 185–191.
(44) Voropai, E. S.; Samtsov, M. P.; Kaplevskii, K. N.; Maskevich, A. A.; Stepuro, V. I.; Povarova, O. I.; Kuznetsova, I. M.; Turoverov, K. K.; Fink, A. L.; Uverskii, V. N. *J. Appl. Spectrosc.* **2003**, *70*, 868–874.
(45) Uversky, V. N.; Winter, S.; Lober, G. *Biophys. Chem.* **1996**, *60*, 79–88.
(46) Pelton, J. H.; McLean, L. R. *Anal. Biochem.* **2000**, *277*, 167–176.
(47) Weert, M. V.; Harris, P. I. *Anal. Biochem.* **2001**, *297*, 160–169.
(48) Dignam, J. D.; Qu, X.; Chaires, J. B. *J. Biol. Chem.* **2001**, *276*, 4028–4037.

JP712026M